DALTON
FULL PAPER

Supramolecular anion binding by the $[ZnCl(Hpz^tBu)_3]^+$ cation (Hpz^tBu = 5-*tert*-butylpyrazole)

Sylvie L. Renard, Colin A. Kilner, Julie Fisher and Malcolm A. Halcrow *

Department of Chemistry, University of Leeds, Woodhouse Lane, Leeds, UK LS2 9JT.
E-mail: M.A.Halcrow@chem.leeds.ac.uk

Received 1st August 2002, Accepted 24th September 2002
First published as an Advance Article on the web 22nd October 2002

Reaction of $ZnCl_2$ with three molar equivalents of 3{5}-*tert*-butylpyrazole (Hpz^tBu) yields $[ZnCl(Hpz^tBu)_3]Cl$ (**1**). Treatment of **1** with an appropriate Ag(I) or Tl(I) salt gives $[ZnCl(Hpz^tBu)_3]X$ ($X^- = BF_4^-$, **4**; $X^- = ClO_4^-$, **5**; $X^- = NO_3^-$, **6**; $X^- = CF_3SO_3^-$, **7**; $X^- = PF_6^-$, **8**). Crystal structures of all of the complexes show a $[ZnCl(Hpz^tBu)_3]^+$ cation, with (for **1** and **4**-**7**) only small deviations from C_{3v} symmetry, with the *tert*-butyl groups forming a bowl-shaped cavity on one face of the complex. The X^- anion binds within this cavity, *via* hydrogen bonding to the three pyrazole N–H groups. For **8**, the PF_6^- guest only interacts with two N–H donors, the third pyrazole ring being twisted away from the anion. We attribute this to steric repulsions between the third ligand and the PF_6^- anion, which is larger than the other guests used in this study. ^1H, ^{13}C and ^{19}F NMR, ESMS and IR studies provide good circumstantial evidence for these structures being retained in solution, although the guest anions undergo rapid intermolecular exchange by NMR that cannot be frozen out above 190 K.

Introduction

The design of ligands for anions is a field of coordination chemistry that is still developing.[1,2] Anion-selective ligands have potential uses as sensors for biomedical and environmental applications.[2] However, the design of receptors that will bind an anion strongly, and prediction of the geometry of bonding interactions to an anion guest, are still challenging tasks. An important extension of this work is to ditopic ligands that can bind simultaneously to the cation(s) and anion(s) of a metal salt. While there are several such ditopic ligand systems for main group metal salts,[3] it is only recently that ligands for transition metal salts have been developed.[4–10] These can have applications in hydrometallurgy and the removal of metals from effluent.

With this in mind, we have recently communicated that complexation of ZnX_2 ($X^- = Cl^-$, Br^-, I^-) by 3{5}-*tert*-butylpyrazole (Hpz^tBu) yields $[ZnX(Hpz^tBu)_3]X$ ($X^- = Cl^-$, **1**; $X^- = Br^-$, **2**; $X^- = I^-$, **3**).[9] The crystal structures of **1**–**3** show a distorted tetrahedral Zn(II) complex cation, whose *tert*-butyl groups are oriented so as to form a shallow bowl-shaped pocket (Fig. 1). The charge-balancing X^- anion lies within this cavity, forming hydrogen bonds to the three pyrazole N–H groups. The related chloride ion guest complex $[HB(Hpz^tBu)_3]Cl[AlCl_4]$ has also been crystallographically characterised.[11] ^1H NMR spectra of **1**–**3** in different solvents, in the presence or absence of $N^nBu_4BF_4$, strongly suggested that these anion-bound structures are retained in solution.[9] As an extension of this initial work, we now present a wider investigation of the anion-binding capabilities of the $[ZnCl(Hpz^tBu)_3]^+$ fragment, in the solid state and in solution.

Results and discussion

Syntheses and crystal structures

Complex **1** does not react cleanly with $NaBF_4$, $NaClO_4$ or NH_4PF_6 in CH_2Cl_2 or MeCN at room temperature or under reflux. However, treatment of solutions of preformed **1** with appropriate Ag(I) or Tl(I) salts affords $[ZnCl(Hpz^tBu)_3]X$ ($X^- = BF_4^-$, **4**; $X^- = ClO_4^-$, **5**; $X^- = NO_3^-$, **6**; $X^- = CF_3SO_3^-$, **7**; $X^- = PF_6^-$, **8**). All of the complexes contain Hpz^tBu and the appropriate X^- anion by IR spectroscopy, while electrospray mass spectrometry showed in each case a strong peak at m/z = 471 from $[^{64}Zn^{35}Cl(Hpz^tBu)_3]^+$. Importantly, no mass peaks corresponding to $[^{64}ZnX(Hpz^tBu)_3]^+$ were detected, strongly suggesting that the X^- counterion does not displace the Cl^- ligand at Zn in the MeOH matrix.

Single crystal X-ray structures were obtained from crystals of stoichiometry **4**·CH_2Cl_2, **5**·$CHCl_3$, **6**, **7**·0.5C_7H_8 and **8**·CH_2Cl_2. During the course of this work a new, unsolvated crystal form of **1** was also obtained and analysed. The Zn centres in **1** and **4**–**7** are very similar, and have approximate C_{3v} symmetry (Fig. 1–5). Metric parameters at Zn for **1** are listed in Table 1; corresponding data for **4**–**7** are available in the ESI. The Zn–Cl bond lengths in these compounds range from 2.2196(4)–2.2469(7) Å, while Zn–N distances are 2.002(3)–2.026(2) Å. There are some deviations from the ideal tetrahedral value in

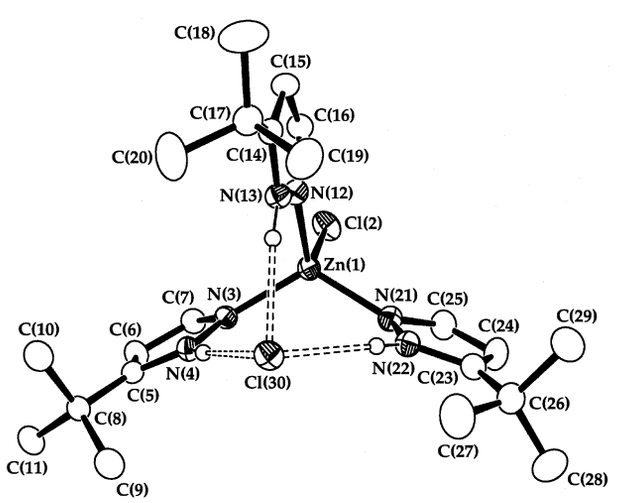

Fig. 1 View of the $[ZnCl(Hpz^tBu)_3]Cl$ moiety in the crystal structure of **1**, showing the atom numbering scheme employed. Thermal ellipsoids are drawn at the 50% probability level. For clarity, all C-bound H atoms have been omitted.

 DOI: 10.1039/b207541p

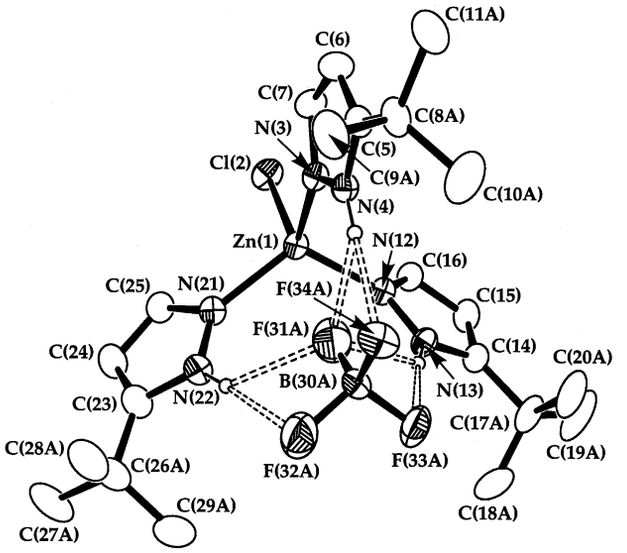

Fig. 2 View of the $[ZnCl(Hpz^tBu_3)]BF_4$ moiety in the crystal structure of $\mathbf{4}\cdot CH_2Cl_2$, showing the atom numbering scheme employed. Details as for Fig. 1. Only one orientation of the disordered *tert*-butyl groups and BF_4^- anion is shown.

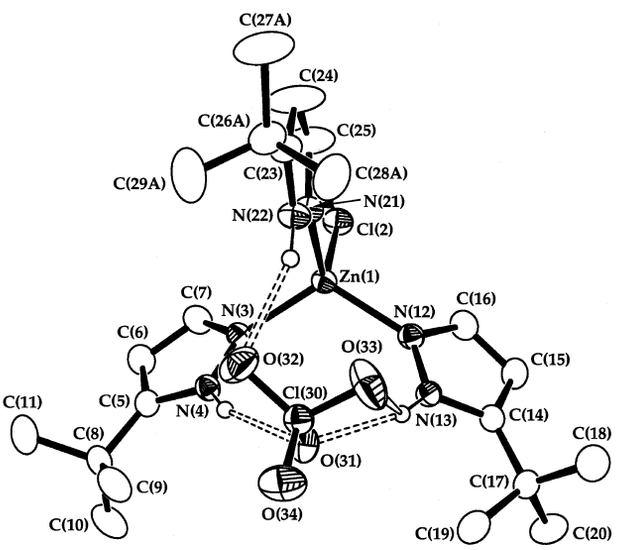

Fig. 3 View of the $[ZnCl(Hpz^tBu_3)]ClO_4$ moiety in the crystal structure of $\mathbf{5}\cdot CHCl_3$, showing the atom numbering scheme employed. Details as for Fig. 1. Only one orientation of the disordered *tert*-butyl groups is shown.

Table 1 Selected bond lengths (Å) and angles (°) for the crystal structure of $[ZnCl(Hpz^tBu_3]Cl$ (**1**)

Zn(1)–Cl(2)	2.2196(4)
Zn(1)–N(3)	2.0108(12)
Zn(1)–N(12)	2.0200(12)
Zn(1)–N(21)	2.0184(12)
Cl(2)–Zn(1)–N(3)	105.66(4)
Cl(2)–Zn(1)–N(12)	107.62(4)
Cl(2)–Zn(1)–N(21)	108.99(4)
N(3)–Zn(1)–N(12)	109.11(5)
N(3)–Zn(1)–N(21)	118.29(5)
N(12)–Zn(1)–N(21)	106.78(5)

the N–Zn–N angles, however, which range between 106.78(5)–119.88(16) Å between the compounds. Importantly, for **1** (Table 1) the bond angles at Zn are crystallographically equal to those in the solvated $\mathbf{1}\cdot 0.5C_5H_{12}$.[9] This implies that the distortion from C_{3v} symmetry in this compound is a genuine consequence of the N–H ··· Cl hydrogen bonding, rather than

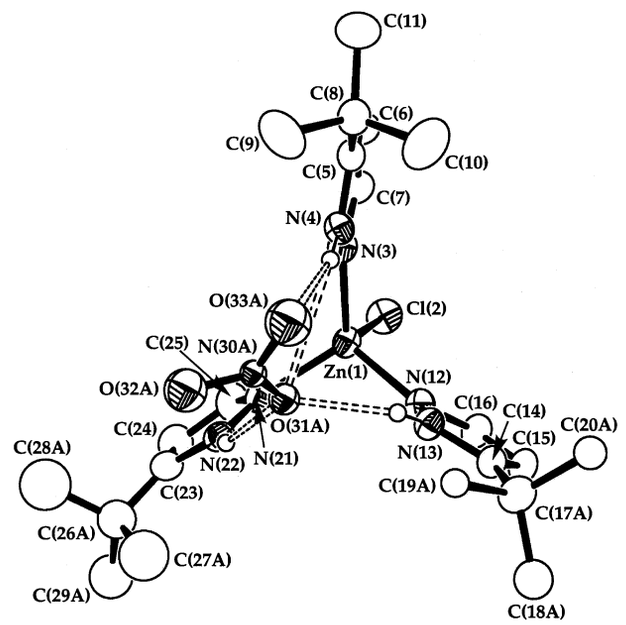

Fig. 4 View of the $[ZnCl(Hpz^tBu_3)]NO_3$ moiety in the crystal structure of **6**, showing the atom numbering scheme employed. Details as for Fig. 1. Only one orientation of the disordered *tert*-butyl groups and NO_3^- is shown.

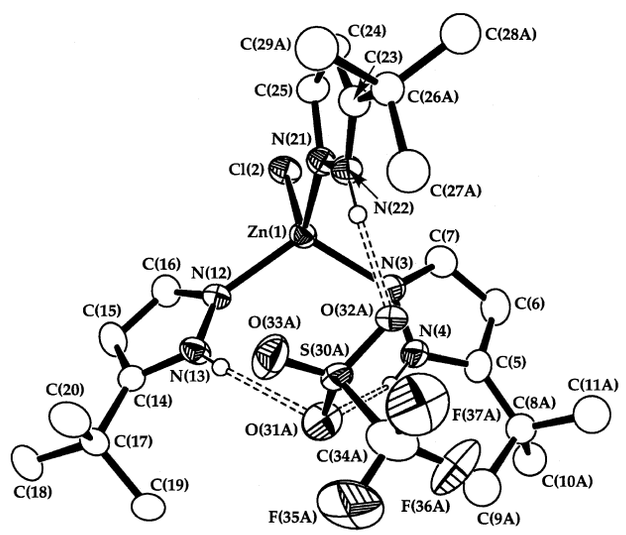

Fig. 5 View of the $[ZnCl(Hpz^tBu_3)]CF_3SO_3$ moiety in the crystal structure of $\mathbf{7}\cdot 0.75CH_2Cl_2$, showing the atom numbering scheme employed. Details as for Fig. 1. Only one orientation of the disordered *tert*-butyl groups and $CF_3SO_3^-$ anion is shown.

simply arising from intermolecular steric interactions in the crystal lattice. Unfortunately, the guest anions in the crystal structures of **4**, **6** and **7**, and one of the two unique anions in **8**, are disordered. Hence, while the connectivity of host–guest hydrogen bonding in these compounds has been reliably determined, detailed discussion of the geometries of their disordered hydrogen bonds is not appropriate.

For **4**–**7**, all three pyrazole ligands hydrogen bond to the X^- anions, although the topology of the hydrogen bonds varies from compound to compound (Scheme 1). In **4**, the disordered BF_4^- ion fits snugly into the cavity, with one B–F bond oriented along the Cl(2)–Zn(1) ··· BF_4^- vector (Fig. 2). Each N–H group forms a bifurcated hydrogen bond, to F(31A) [or F(31B) in the other disorder orientation] and to one other F atom. Both partially occupied BF_4^- sites show this mode of hydrogen-bonding. The ClO_4^- ion in **5** is crystallographically ordered. Two N–H groups of the receptor molecule hydrogen-bond to the same O atom; one of these donors also forms a weaker

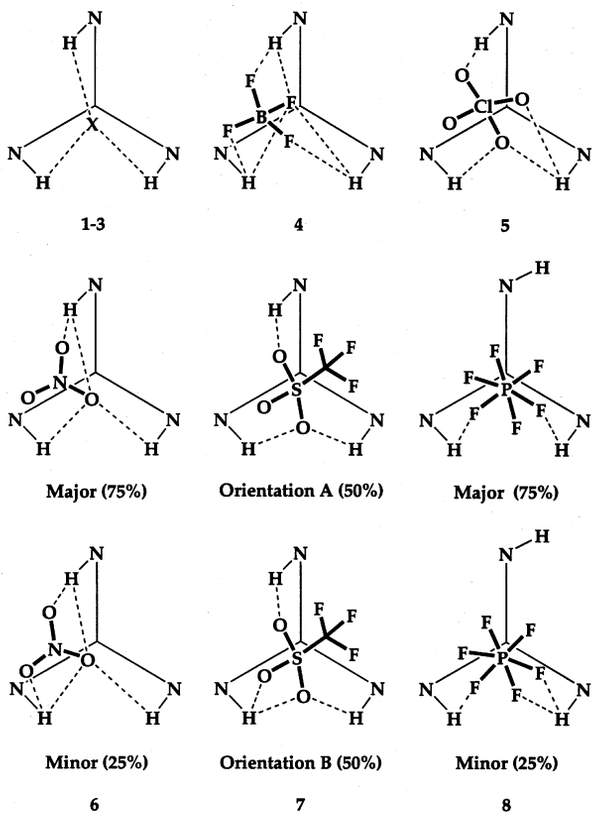

Scheme 1 The different hydrogen-bonding geometries between the $[ZnY(Hpz^tBu)_3]^+$ (**1** and **4**–**8**, $Y^- = Cl^-$; **2**, $Y^- = Br^-$; **3**, $Y^- = I^-$) receptor and the guest anion in the crystal structures of **1**–**8**.

Table 2 Uncorrected metric parameters for the hydrogen bonds present in the crystal structure of $[ZnCl(Hpz^tBu)_3]ClO_4{\cdot}CHCl_3$ [**5**·$CHCl_3$; lengths (Å), angles (°)]

	H ··· O	N ··· O	N–H ··· O
N(4)–H(4) ··· O(31)	2.03	2.859(2)	155.8
N(13)–H(13) ··· O(31)	2.07	2.890(2)	155.4
N(13)–H(13) ··· O(33)	2.64	3.314(3)	133.9
N(22)–H(22) ··· O(32)	2.15	2.972(2)	155.6

bifurcated interaction to a second O atom. The third N–H group interacts with a different O atom (Fig. 3, Table 2, Scheme 1). We ascribe the different binding modes of BF_4^- in **4** and ClO_4^- in **5** to the larger radius of the ClO_4^- ion,[12] which is a less good fit for the anion-binding cavity of the complex receptor.

The NO_3^- ion in **6** is badly disordered, over four orientations. Three of the partial NO_3^- molecules adopt the same pattern of hydrogen-bonding, with all three N–H groups interacting with the same O atom, and one forming a bifurcated hydrogen bond to a second O atom (Fig. 4). The fourth disorder orientation is similar, but with an additional bifurcated hydrogen bond to the third nitrate O atom (Scheme 1). The $CF_3SO_3^-$ ion in **7** also disordered, over two orientations that were modelled as equally occupied. Only two O atoms of one orientation interact with the receptor N–H groups (Fig. 5, Scheme 1). However, in the other orientation one N–H group forms a bifurcated hydrogen bond to the third triflate O atom, in the same manner as for the ClO_4^- ion in **5**.

Crystals of **8**·CH_2Cl_2 contain two formula units per asymmetric unit, although there are only small structural differences between the two independent complex cations (Table 3). As for **1**–**7**, the PF_6^- anions in **8** lie within the cavities formed by the Hpz^tBu ligands of the complex cations. However, in contrast to **1**–**7**, only two of the three N–H groups of each receptor form hydrogen bonds to this anion (Fig. 6, Table 4, Scheme 1). The

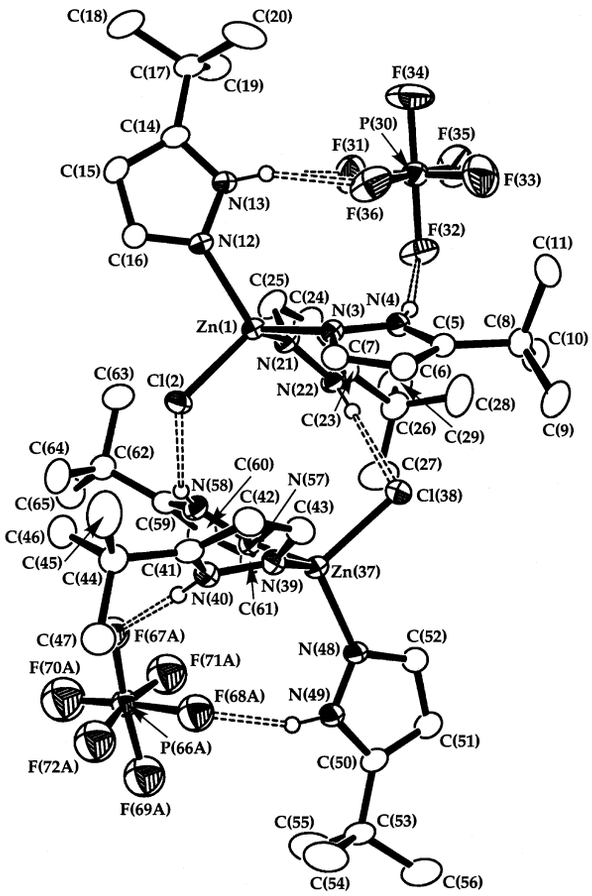

Fig. 6 View of the two crystallographically independent $[ZnCl(Hpz^tBu)_3]PF_6$ moieties in the crystal structure of **8**·CH_2Cl_2, showing the atom numbering scheme employed. Details as for Fig. 1. Only one orientation of the disordered PF_6^- anion is shown.

third Hpz^tBu ligand has rotated about its Zn–N bond, so the pyrazole ring is almost perpendicular to the Zn ··· PF_6^- vector, and instead hydrogen bonds to the Cl^- ligand from the other unique molecule (Table 4). Hence, **8** associates into hydrogen bonded dimers in the crystal (Fig. 6). Space-filling models imply that this structure is imposed by the larger cone-angle of the PF_6^- ion, which is in van der Waals contact with the 'perpendicular' pyrazole ring. Presumably, steric repulsions between the PF_6^- guest and *tert*-butyl group cause the latter to be displaced away from the anion-binding cavity. Despite these differences, the bond lengths and angles at Zn in **8** still lie with the ranges shown by **1** and **4**–**7**, to within 3 s.u.s (Table 3).

NMR properties of the compounds

Unless otherwise stated, all NMR studies in this work were carried out in $CDCl_3$. The ^1H and ^{13}C NMR spectra of **1**–**8** at 290 K all show the presence of a single Hpz^tBu environment. This is consistent with the crystal structures of **1**–**4**, but not of **5**–**8**. The raised NMR symmetry of **5**–**8** is a consequence of rapid intermolecular exchange of the anion guest (see below). The spectra of the different compounds show some differences, particularly in the chemical shift of the N–H proton resonance (δ_{NH}; Fig. 7). The fact that δ_{NH} depends on X^- in $[ZnCl(Hpz^tBu)_3]X$ suggests that N–H ··· X hydrogen bonding is important in the solution structures of **1**–**8**. There is an approximate correlation of δ_{NH} with the identity of the hydrogen-bond acceptor atom in the guest anion (Fig. 7):

halide [Cl^-, Br^-, I^-] ≥ O [NO_3^-, ClO_4^-, $CF_3SO_3^-$] > F [BF_4^-, PF_6^-]

Table 3 Selected bond lengths (Å) and angles (°) for the two independent molecules in the crystal structure of $[ZnCl(Hpz^tBu)_3]PF_6 \cdot CH_2Cl_2$ ($\mathbf{8} \cdot CH_2Cl_2$)

Zn(1)–Cl(2)	2.2349(8)	Zn(37)–Cl(38)	2.2486(8)
Zn(1)–N(3)	1.994(2)	Zn(37)–N(39)	1.994(3)
Zn(1)–N(12)	2.020(2)	Zn(37)–N(48)	2.009(2)
Zn(1)–N(21)	2.006(3)	Zn(37)–N(57)	2.010(2)
Cl(2)–Zn(1)–N(3)	106.01(7)	Cl(38)–Zn(37)–N(39)	106.36(8)
Cl(2)–Zn(1)–N(12)	103.38(8)	Cl(38)–Zn(37)–N(48)	106.34(8)
Cl(2)–Zn(1)–N(21)	119.62(8)	Cl(38)–Zn(37)–N(57)	109.11(8)
N(3)–Zn(1)–N(12)	118.35(10)	N(39)–Zn(37)–N(48)	119.07(11)
N(3)–Zn(1)–N(21)	107.92(10)	N(39)–Zn(37)–N(57)	109.34(11)
N(12)–Zn(1)–N(21)	102.26(10)	N(48)–Zn(37)–N(57)	106.31(11)

Table 4 Uncorrected metric parameters for the hydrogen bonds present in the crystal structure of $[ZnCl(Hpz^tBu)_3]PF_6 \cdot CH_2Cl_2$ [$\mathbf{8} \cdot CH_2Cl_2$; lengths (Å), angles (°)]. Hydrogen bonds to the disordered anion [P(66A)–F(72A) in Fig. 6] are not listed

	H ··· X	N ··· X	N–H ··· X
N(4)–H(4) ··· F(32)[a]	2.09	2.942(3)	163.4
N(13)–H(13) ··· F(31)[a]	2.44	3.196(4)	144.6
N(13)–H(13) ··· F(36)[a]	2.18	2.976(4)	150.9
N(22)–H(22) ··· Cl(38)[b]	2.40	3.277(3)	174.0
N(58)–H(58) ··· Cl(2)[b]	2.41	3.215(3)	151.6

[a] X = F. [b] X = Cl.

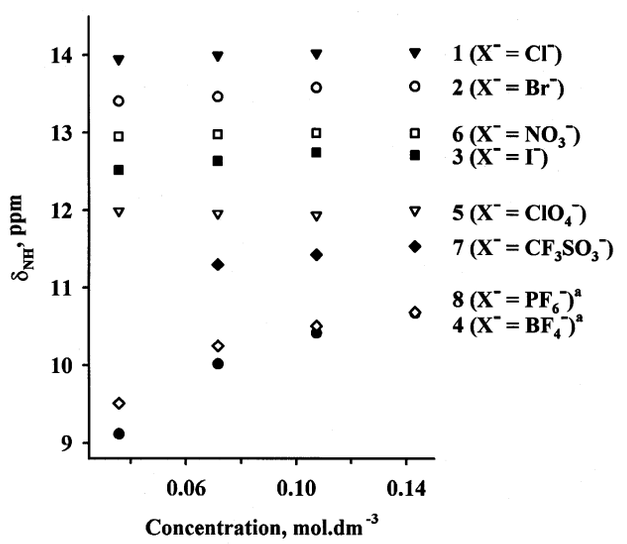

Fig. 7 Concentration dependence of δ_{NH} in $CDCl_3$ at 293 K for **1**–**8**. There is no data point at 0.036 mol dm^{-3} for **7**, because the N–H resonance was so broad that δ_{NH} could not be measured accurately. The black circle points correspond to **4**, while the open diamonds are from **8**. At 0.143 mol dm^{-3}, the data points from these two compounds overlie each other.

Within the halides and oxyanion series, there is a direct correlation between δ_{NH} and the pK_a of the conjugate acid of each anion (Fig. 7), which follow the following trends in aqueous solution:[13–15]

$$HCl\ (-7) > HBr\ (-9) > HI\ (-11)$$
$$HNO_3\ (ca.\ -1) > HClO_4\ (ca.\ -9) > CF_3SO_3H\ (-11)$$

This is reasonable, since a more basic anion should form stronger hydrogen bonds to the receptor complex which would in turn lead to a higher value of δ_{NH}. It is uncertain whether the fluoroanions also follow this trend, since HBF_4 and HPF_6 are fully dissociated in water so that accurate pK_a values are not available.[13,15]

For **2**–**4**, **7** and **8** δ_{NH} increases with increasing concentration between 0.036–0.143 mol dm^{-3}, reaching a plateau at higher concentrations (Fig. 7). This demonstrates that these five compounds are in equilibrium in solution, most likely reflecting only partial binding of the guest anion ['X', eqn. (1)]:

$$\{[ZnCl(Hpz^tBu)_3]X\} \rightleftharpoons [ZnCl(Hpz^tBu)_3]^+ + X^- \quad (1)$$

This dependence is markedly more pronounced for **4** and **8** than for the other compounds (Fig. 7), strongly suggesting that BF_4^- and PF_6^- bind much more weakly to $[ZnCl(Hpz^tBu)_3]^+$ than the halide or oxyanions in this study. In contrast **1**, **5** and **6** do not undergo a detectable equilibrium under these conditions, implying that these compounds bind their guest anions more strongly. All the other ^{1}H and ^{13}C chemical shifts for **1**–**8** are essentially independent of concentration. Importantly, in all cases the resonances for C^3 and C^5 of the pyrazole ring are sharp, and have comparable intensity to that of the peak corresponding to C^4. This implies that intermolecular exchange of Hpz^{t}Bu between Zn centres is not occurring significantly under these conditions.[9,16]

As we have previously reported, addition of an excess of the appropriate N^nBu_4X ($X^- = Cl^-$, Br^-, I^-) salt to NMR solutions of **1**–**3** induces fluxionality at the Zn centres, as evidenced by broadening of the C^3 and C^5 ^{13}C NMR peaks.[9] We attributed this to the nucleophilicity of the added halide, which could promote ligand exchange by attacking the Zn centres. In contrast, addition of one molar equivalent of dry $N^nBu_4BF_4$ to **4**, $N^nBu_4NO_3$ to **6**, $N^nBu_4CF_3SO_3$ to **7** and $N^nBu_4PF_6$ to **8** did not induce analogous changes in their ^{13}C NMR spectra. This shows that these anions cannot promote intermolecular ligand exchange in these compounds, which is consistent with their poorer nucleophilicity compared to the halides. Addition of the relevant N^nBu_4X salt to concentrated solutions of **4** and **6**–**8** also caused little or no change in δ_{NH}, or any other ^{1}H resonance. This is additional evidence for strong binding of these anions to the intact zinc receptor under these conditions. Similar measurements were not attempted for **5**, because of the difficulty in obtaining rigorously dry $N^nBu_4ClO_4$.

The ^{19}F spectra of **4** and **8** both show a single resonance, at δ −147.5 (**4**) and −69.4 ppm (**8**). These chemical shifts are different from those of $N^nBu_4BF_4$ (−152.2) or $N^nBu_4PF_6$ (−72.6) under the same conditions, which can again be attributed to binding of BF_4^- or PF_6^- to $[ZnCl(Hpz^tBu)_3]^+$ in $CDCl_3$. Addition of one molar equivalent of $N^nBu_4BF_4$ to **4**, or $N^nBu_4PF_6$ to **8**, afforded spectra again showing only one anion environment, with a chemical shift close to the average of the shifts for the two constituent salts in the sample. Thus, **4** + $N^nBu_4BF_4$ yields a peak at −149.6, and **8** + $N^nBu_4PF_6$ a peak at −70.5 ppm. This demonstrates that the guest anions in **4** and **8** undergo rapid intermolecular exchange on the NMR timescale. This is consistent with the ^{1}H NMR data on these compounds, which strongly suggest that free and bound BF_4^- or PF_6^- are in equilibrium in this solvent (see above).

Variable temperature ^{1}H NMR studies were carried out on **1**, **4** and **8** in $CDCl_3$. Partial decoalescence of the pyrazole ring H atom resonances was reached near 220 K for all three complexes, consistent with the intermolecular exchange of the guest anion that was demonstrated above. However, the slow

exchange limit was not reached for either compound within the liquid range of $CDCl_3$. Similar studies in C_7D_8 also did not give complete decoalescence above 190 K. This has meant that detailed measurements of the association constant between $[ZnCl(Hpz^tBu)_3]^+$ and Cl^-, BF_4^- or PF_6^- have not been possible.

Concluding remarks

These studies have shown that the $[ZnCl(Hpz^tBu)_3]^+$ receptor is able to bind a range of anions in the solid state, whose effective radii range from 1.8 Å for Cl^- [2] to 2.3 Å for PF_6^-.[12] In all cases the bound anions lie within the cavity formed by the Hpz^tBu *tert*-butyl groups although, unsurprisingly, the modes of hydrogen bonding of the receptor to the anion varies from compound to compound. The crystal structure of **8** shows that PF_6^- is too large to fit within the hydrophobic cavity of $[ZnCl(Hpz^tBu)_3]^+$ without causing substantial structural distortions, and it is likely that larger anions than PF_6^- will bind to this receptor more weakly.

The ^{13}C NMR data in this work and ref. 9 demonstrate that intermolecular exchange of Hpz^tBu occurs for **1**–**8** in $CDCl_3$ to only a small degree. In addition, ^1H NMR shows that the chemical environment of their N–H protons in $CDCl_3$ is very dependent on the identity of the guest anion. These observations are good evidence for the retention of the solid-state structures upon dissolution of **1**–**8**, and hence for anion-binding in this solvent. Consistent with this, anion binding in **4** and **8** has been directly observed by ^{19}F NMR. The high affinity of $[ZnCl(Hpz^tBu)_3]^+$ for monoanions is reasonable, since its positive charge, multiple hydrogen-bond donors and hydrophobic pocket should all combine to promote these host–guest interactions.[2] Although we have not been able to measure any binding constants in our system, from the concentration dependence of δ_{NH} for **1**–**8** we can rank the different anions in order of their relative affinities for the $[ZnY(Hpz^tBu)_3]^+$ (Y^- = Cl^-, Br^-, I^-) receptor:

$$[Cl^-, ClO_4^-, NO_3^-] > [Br^-, I^-, CF_3SO_3^-] >> [BF_4^-, PF_6^-]$$

Although extrapolation of aqueous acid/base behaviour to non-aqueous systems is not always valid,[17] it is noteworthy that this ordering correlates approximately with the basicity of these anions in aqueous solution (see above). In particular, the crystal structure of **4** shows that the size and shape of BF_4^- compliments the $[ZnCl(Hpz^tBu)_3]^+$ host better than any of the other anions studied. Hence, it appears that the affinity of different anions for $[ZnCl(Hpz^tBu)_3]^+$ is governed predominantly by their hydrogen-bond acceptor capability, rather than by their steric complimentarity with the receptor cavity.

We are presently examining the structures of salts of $[ZnCl(Hpz^tBu)_3]^+$ with other, more globular anions. These are of interest for their solid-state structures, and because they may form only weak host–guest complexes in solution. That would allow us to study in more detail the affinity of our receptor for the anions in this study, or for other guests. The ready availability of 3- and 5-substituted pyrazoles also provides great scope for varying the steric properties and hydrogen bond-topology within the cavity of our receptor, and for attaching a reporter group to its periphery that may allow its use as an anion sensor. We are also pursuing these possibilities.

Experimental

Unless stated otherwise, all manipulations were performed in air using commercial grade solvents. Hpz^tBu [18] and **1**–**3** [9] were prepared according to the published methods, while $AgBF_4$, $AgClO_4$, $AgNO_3$, $AgCF_3SO_3$ and $TlPF_6$ were used as supplied.

Syntheses of 4–8

The syntheses of all of these complexes followed the same basic procedure, as described here for **4**. A mixture of $ZnCl_2$ (0.37 g, 2.6×10^{-3} mol) and Hpz^tBu (1.00 g, 8.0×10^{-3} mol) in MeOH (50 cm^3) was stirred until all the solid had dissolved. A solution of $AgBF_4$ (0.52 g, 2.6×10^{-3} mol) in MeOH (10 cm^3) was then added, and the mixture stirred for 30 min. The mixture was filtered, and the filtrate evaporated to dryness. The white residue was redissolved in a minimum volume of CH_2Cl_2, and a large excess of pentane added to the colourless solution. Storage at −30 °C gave colourless crystals of the product. Similar reactions using equivalent amounts of $AgClO_4$, $AgNO_3$, $AgCF_3SO_3$ or $TlPF_6$ afforded **5**–**8**. Yields ranged from 55–82%. [**CAUTION!** While we have experienced no difficulty in handling **5**, metal–organic perchlorates are potentially explosive and should be handled with due care in small quantities].

For $[ZnCl(Hpz^tBu)_3]BF_4$ (**4**): found C,44.7; H, 6.5; N, 15.2%. Calcd. for $C_{21}H_{36}BClF_4N_6Zn$ C, 45.0; H, 6.5; N, 15.0%. Electrospray mass spectrum: *m*/*z* 471 $[^{64}Zn^{35}Cl(Hpz^tBu)_3]^+$. NMR spectra ($CDCl_3$): ^1H δ 10.68 (br s, 3H, N*H*), 8.05 (d, 2.3 Hz, 3H, pz H^3), 6.24 (d, 2.3 Hz, 3H, pz H^4), 1.37 (s, 18H, CCH_3). $^{13}C\{^1H\}$ δ 156.8 (s, pz C^5), 142.1 (s, pz C^3), 102.9 (s, pz C^4), 31.3 (s, CCH_3), 29.7 (s, CCH_3). ^{19}F δ −147.5 (s, BF_4^-). IR spectrum (nujol): 3363m, 1559m, 1303m, 1204w, 1160m, 1114s, 1060vs, 982m, 955s, 796m cm^{-1}.

For $[ZnCl(Hpz^tBu)_3]ClO_4$ (**5**): found C, 44.1; H, 6.3; N, 14.9%. Calcd. for $C_{21}H_{36}Cl_2N_6O_4Zn$ C, 44.0; H, 6.3; N, 14.7%. Electrospray mass spectrum: *m*/*z* 471 $[^{64}Zn^{35}Cl(Hpz^tBu)_3]^+$. NMR spectra ($CDCl_3$): ^1H δ 11.96 (br s, 3H, N*H*), 8.07 (d, 2.3 Hz, 3H, pz H^3), 6.24 (d, 2.3 Hz, 3H, pz H^4), 1.39 (s, 18H, CCH_3). $^{13}C\{^1H\}$ δ 157.0 (s, pz C^5), 142.3 (s, pz C^3), 102.9 (s, pz C^4), 31.4 (s, CCH_3), 29.8 (s, CCH_3). IR spectrum (nujol): 3279m, 1560m, 1303m, 1207w, 1153m, 1119m, 1090vs, 1030m, 990s, 958s, 796m cm^{-1}.

For $[ZnCl(Hpz^tBu)_3]NO_3$ (**6**): found C, 47.2; H, 6.7; N, 18.4%. Calcd. for $C_{21}H_{36}ClN_7O_3Zn$ C, 47.1; H, 6.8; N, 18.3%. Electrospray mass spectrum: *m*/*z* 471 $[^{64}Zn^{35}Cl(Hpz^tBu)_3]^+$. NMR spectra ($CDCl_3$): ^1H δ 12.97 (br s, 3H, N*H*), 7.96 (d, 2.2 Hz, 3H, pz H^3), 6.21 (d, 2.2 Hz, 3H, pz H^4), 1.38 (s, 18H, CCH_3). $^{13}C\{^1H\}$ δ 156.6 (s, pz C^5), 141.6 (s, pz C^3), 102.7 (s, pz C^4), 31.3 (s, CCH_3), 29.9 (s, CCH_3). IR spectrum (nujol): 3191m, 3168m, 1563m, 1317m, 1207w, 1158m, 1114m, 1035m, 994m, 953s, 805m cm^{-1}.

For $[ZnCl(Hpz^tBu)_3]CF_3SO_3$ (**7**): found C, 42.3; H, 5.9; N, 13.4%. Calcd. for $C_{22}H_{36}ClF_3N_6O_3SZn$ C, 42.5; H, 5.8; N, 13.5%. Electrospray mass spectrum: *m*/*z* 471 $[^{64}Zn^{35}Cl(Hpz^tBu)_3]^+$. NMR spectra ($CDCl_3$): ^1H δ 11.64 (br s, 3H, N*H*), 8.04 (d, 2.3 Hz, 3H, pz H^3), 6.22 (d, 2.3 Hz, 3H, pz H^4), 1.37 (s, 18H, CCH_3). $^{13}C\{^1H\}$ δ 156.9 (s, pz C^5), 142.0 (s, pz C^3), 119.9 (q, 318.1 Hz, $CF_3SO_3^-$), 102.9 (s, pz C^4), 31.4 (s, CCH_3), 29.8 (s, CCH_3). IR spectrum (nujol): 3278m, 3196w, 1567m, 1304s, 1233m, 1203m, 1168m, 1117m, 1025s, 989m, 958s, 809m cm^{-1}.

For $[ZnCl(Hpz^tBu)_3]PF_6$ (**8**): found C, 40.6; H, 5.7; N, 13.8%. Calcd. for $C_{22}H_{36}ClF_6N_6PZn$ C, 40.8; H, 5.9; N, 13.6%. Electrospray mass spectrum: *m*/*z* 471 $[^{64}Zn^{35}Cl(Hpz^tBu)_3]^+$. NMR spectra ($CDCl_3$): ^1H δ 10.70 (br s, 3H, N*H*), 8.04 (d, 2.3 Hz, 3H, pz H^3), 6.25 (d, 2.3 Hz, 3H, pz H^4), 1.36 (s, 18H, CCH_3). $^{13}C\{^1H\}$ δ 157.1 (s, pz C^5), 142.2 (s, pz C^3), 103.1 (s, pz C^4), 31.3 (s, CCH_3), 29.7 (s, CCH_3). ^{19}F δ −69.4 (d, 717 Hz, PF_6^-). IR spectrum (nujol): 3403m, 3287w, 3156w, 1562w, 1301m, 1256m, 1204m, 1116s, 990m, 840vs cm^{-1}.

Single crystal X-ray structure determinations

All crystals were grown by storage of solutions of the compounds at −30 °C in the following solvents: CH_2Cl_2 (**1**); CH_2Cl_2/pentane (**4**·CH_2Cl_2, **6** and **8**·CH_2Cl_2); $CHCl_3$/pentane

Table 5 Experimental details for the new single crystal structure determinations in this study

	[ZnCl(Hpz′Bu$_3$)Cl] (**1**)	[ZnCl(Hpz′Bu$_3$)]BF$_4$·CH$_2$Cl$_2$ (**4**·CH$_2$Cl$_2$)	[ZnCl(Hpz′Bu$_3$)]ClO$_4$·CHCl$_3$ (**5**·CHCl$_3$)	[ZnCl(Hpz′Bu$_3$)]NO$_3$ (**6**)	[ZnCl(Hpz′Bu$_3$)]CF$_3$SO$_3$·0.5C$_7$H$_8$ (**7**·0.5C$_7$H$_8$)	[ZnCl(Hpz′Bu$_3$)]PF$_6$·CH$_2$Cl$_2$ (**8**·CH$_2$Cl$_2$)
Formula	$C_{21}H_{36}Cl_2N_6Zn$	$C_{22}H_{38}BCl_3F_4N_6Zn$	$C_{22}H_{37}Cl_5N_6O_4Zn$	$C_{21}H_{36}ClN_7O_3Zn$	$C_{25.5}H_{40}ClF_3N_6O_3SZn$	$C_{22}H_{38}Cl_3F_6N_6PZn$
M_r	508.83	645.11	6592.20	535.39	668.52	703.27
Crystal system	monoclinic	monoclinic	monoclinic	monoclinic	monoclinic	triclinic
Space group	$P2_1/c$	$P2_1/c$	$P2_1/c$	$P2_1/c$	$P2_1/c$	$P\bar{1}$
a/Å	17.2537(3)	17.5359(3)	9.9363(1)	17.7119(8)	10.2895(1)	14.4475(2)
b/Å	10.6738(1)	10.7282(2)	10.0965(1)	10.3815(4)	10.8281(1)	14.7862(2)
c/Å	14.6666(2)	18.5742(3)	31.8586(4)	14.9451(5)	29.3462(4)	15.1702(2)
α/°	–	–	–	–	–	90.2896(5)
β/°	103.7416(5)	116.4774(6)	96.7932(7)	101.0915(15)	94.4541(5)	91.5739(5)
γ/°	–	–	–	–	–	96.3712(7)
V/Å^3	2623.72(6)	3127.83(9)	3173.68(6)	2696.72(18)	3254.83(6)	3219.38(8)
Z	4	4	4	4	4	4
μ/mm^{-1}	1.158	1.087	1.232	1.044	0.953	1.119
T/K	150(2)	150(2)	150(2)	150(2)	150(2)	150(2)
Measured reflections	31333	30436	25384	15625	33103	59093
Independent reflections	7681	7131	7236	6115	7452	14762
R_{int}	0.049	0.067	0.073	0.063	0.049	0.085
$R(F)^a$, $wR(F^2)^b$	0.033, 0.088	0.052, 0.150	0.037, 0.105	0.076, 0.184	0.038, 0.105	0.055, 0.162
S	1.026	1.051	1.051	1.095	1.023	1.022

^{a} $R = \Sigma[|F_o| - |F_c|]/\Sigma|F_o|$. ^{b} $wR = [\Sigma w(F_o^2 - F_c^2)/\Sigma wF_o^4]^{1/2}$. ^{c} $P = (F_o^2 + 2F_c^2)/3$.

(**5**·CHCl$_3$); and toluene/pentane (**7**·0.5C$_7$H$_8$). Experimental details for these structure determinations are listed in Table 5. All structures were solved by direct methods (SHELXS 86[19]) and refined by full matrix least-squares on F^2 (SHELXL 97[20]), with H atoms placed in calculated positions.

CCDC reference numbers 191073–191078.

See http://www.rsc.org/suppdata/dt/b2/b207541p/ for crystallographic data in CIF or other electronic format.

X-Ray structure determination of 1. No disorder was detected during refinement of this structure, and no restraints were applied. All H atoms were placed in calculated positions and all non-H atoms were refined anisotropically.

X-Ray structure determination of 4·CH$_2$Cl$_2$. All three *tert*-butyl groups in the molecule were found to be disordered during refinement; one over two orientations with a 0.60 : 0.40 occupancy ratio; one over two orientations with a 0.70 : 0.30 occupancy ratio; and one over three orientations with occupancies of 0.50, 0.30 and 0.20, two of which share a common quaternary C atom. The BF_4^- anion is also disordered, over two equally occupied orientations. Finally, the occluded solvent is also badly disordered, and lies near a crystallographic inversion centre. Four distinct partial CH_2Cl_2 molecules were incorporated into the final model. The following restraints were applied to each individual disorder orientation: C–C = 1.53(2), 1,3-C ··· C = 2.50(2), B–F = 1.36(2), F ··· F = 2.22(2), C–Cl = 1.76(2) and Cl ··· Cl = 2.87(2) Å. All non-H atoms with occupancies > 0.5 were refined anisotropically. All H atoms were placed in calculated positions and refined using a riding model, except for methyl groups belonging to disordered *tert*-butyl groups whose torsions were not refined.

X-Ray structure determination of 5·CHCl$_3$. One *tert*-butyl group in the molecule was disordered over two orientations, with occupancies of 0.60 and 0.40. All disordered C–C bonds were restrained to 1.52(2) Å, and 1,3-C ··· C distances within a given disorder orientation to 2.48(2) Å. All non-H atoms with occupancies > 0.5 were refined anisotropically, and all H atoms were placed in calculated positions and refined using a riding model.

X-Ray structure determination of 6. Two of the three *tert*-butyl groups in the molecule were found to be disordered during refinement: one over three orientations with occupancies of 0.40, 0.30 and 0.30, two of them sharing a common quaternary C atom; and, one over three equally occupied orientations. All disordered C–C bonds were restrained to 1.52(2) Å, and 1,3-C ··· C distances within a given disorder orientation to 2.48(2) Å. The NO_3^- anion is also disordered, over four equally occupied orientations. Each N–O bond was restrained to 1.24(1) Å, and O ··· O distances within a given disorder orientation to 2.15(1) Å. All non-H atoms with occupancies > 0.5 were refined anisotropically. All H atoms were placed in calculated positions and refined using a riding model, except for methyl groups belonging to disordered *tert*-butyl groups whose torsions were not refined.

X-Ray structure determination of 7·0.5C$_7$H$_8$. The asymmetric unit contains one complex cation and one anion, lying on general positions; and, half a molecule of toluene lying across a crystallographic inversion centre. The $CF_3SO_3^-$ anion is disordered, over two equally occupied orientations. The following restraints were applied to each disorder orientation of this anion: S–O = 1.42(1), O ··· O = 2.32(1), S–C = 1.78(1), C–F = 1.31(1), F ··· F = 2.14(1) Å. Two of the three *tert*-butyl groups are also disordered, each over two equally

occupied orientations. These were modelled using the restraints C–C = 1.53(2) Å and 1,3-C ··· C distances within a given disorder orientation = 2.50(2) Å. Finally, the following restraints were applied to the toluene half-molecule: intra-ring C–C = 1.38(2) Å and intra-ring 1,3-C ··· C = 2.41(2) Å. All wholly occupied non-H atoms, plus the two partial $CF_3SO_3^-$ anions, were refined anisotropically. All H atoms were placed in calculated positions and refined using a riding model.

X-Ray structure determination of 8·CH_2Cl_2. The asymmetric unit contains two crystallographically independent complex cations, two PF_6^- anions and two CH_2Cl_2 molecules, all lying on general positions. One of the PF_6^- anions is disordered, over three equally occupied orientations. All P–F bonds within a given disorder orientation were restrained to 1.60(2) Å, *cis*-F ··· F distances to 2.26(2) Å and *trans*-F ··· F distances within a given disorder orientation to 3.20(2) Å. Both CH_2Cl_2 molecules were also disordered. For one of these, one Cl atom was disordered over two partial sites with occupancies of 0.70 : 0.30. All three heavy atoms of the second molecule were disordered over four orientations, with occupancies of 0.55 : 0.15 : 0.15 : 0.15; these can be considered as two pairs in which each partial molecule shares a common Cl atom. All disordered C–Cl bonds were restrained to 1.75(2) Å, and Cl ··· Cl distances within a given disorder orientation to 2.86(2) Å. All non-H atoms with occupancies > 0.5 were refined anisotropically, while all H atoms were placed in calculated positions and refined using a riding model.

Other measurements

Infra-red spectra were obtained using a Nicolet Avatar 360 spectrophotometer, as Nujol mulls pressed between NaCl windows. Electrospray mass spectra were performed on a Micromass LCT TOF spectrometer, employing a MeOH matrix. CHN microanalyses were performed by the University of Leeds Department of Chemistry microanalytical service. All room-temperature ^{1}H (250.1 MHz) and ^{13}C (62.9 MHz) NMR spectra were run on a Bruker ARX250 spectrometer, while ^{19}F spectra (188.3 MHz) were obtained on a Bruker AC200 instrument. Variable temperature ^{1}H spectra were obtained on a Bruker DRX500 spectrometer, operating at 500.1 MHz.

Acknowledgements

The authors gratefully acknowledge funding by The Royal Society (M.A.H.), the EPSRC (S.L.R.) and the University of Leeds.

References

1 (*a*) F. P. Schmidtchen and M. Berger, *Chem. Rev.*, 1997, **97**, 1609; (*b*) P. D. Beer and D. K. Smith, *Prog. Inorg. Chem.*, 1997, **46**, 1; (*c*) M. M. G. Antonisse and D. G. Reinhoudt, *Chem. Commun.*, 1998, 443.
2 P. D. Beer and P. A. Gale, *Angew. Chem., Int. Ed.*, 2001, **40**, 486.
3 M. T. Reetz, *Comprehensive Supramolecular Chemistry*, ed. J. L. Atwood, J. E. D. Davies, D. D. McNicol and F. Vögtle, Elsevier, Oxford, 1996, vol. 2, ch. 18, pp. 553–562.
4 P. D. Beer and J. Cadman, *Coord. Chem. Rev.*, 2000, **205**, 1311.
5 (*a*) D. J. White, N. Laing, H. Miller, S. Parsons, S. Coles and P. A. Tasker, *Chem. Commun.*, 1999, 2077; (*b*) H. A. Miller, N. Laing, S. Parsons, A. Parkin, P. A. Tasker and D. J. White, *J. Chem. Soc., Dalton Trans.*, 2000, 3773.
6 L. H. Uppadine, M. G. B. Drew and P. D. Beer, *Chem. Commun.*, 2001, 291.
7 C. R. Bondy, S. J. Loeb and P. A. Gale, *Chem. Commun.*, 2001, 729.
8 J. B. Love, J. M. Vere, M. W. Glenny, A. J. Blake and M. Schröder, *Chem. Commun.*, 2001, 2678.
9 X. Liu, C. A. Kilner and M. A. Halcrow, *Chem. Commun.*, 2002, 704.
10 Z. Shirin, J. Thompson, L. Liable-Sands, G. P. A. Yap, A. L. Rheingold and A. S. Borovik, *J. Chem. Soc., Dalton Trans.*, 2002, 1714.
11 A. Looney, G. Parkin and A. L. Rheingold, *Inorg. Chem.*, 1991, **30**, 3099.
12 D. M. P. Mingos and A. L. Rohl, *J. Chem. Soc., Dalton Trans.*, 1991, 3419.
13 A. J. Gordon and R. A. Ford, *The Chemist's Companion: A Handbook of Practical Data, Techniques and References*, John Wiley and Sons, New York, 1972, pp. 58–62.
14 P. J. Domaille, J. D. Druliner, L. W. Gosser, J. M. Read, E. R. Schmelzer and W. R. Stevens, *J. Org. Chem.*, 1985, **50**, 189.
15 M. Leuchs and G. Zundel, *Can. J. Chem.*, 1980, **58**, 311.
16 C. Lopez, R. M. Claramunt, S. Trofimenko and J. Elguero, *Can. J. Chem.*, 1993, **71**, 678.
17 See *e.g.*, M. G. Basalotte, J. Durán, M. J. Fernández-Trujillo and M. A. Máñez, *Organometallics*, 2000, **10**, 695.
18 S. Trofimenko, J. C. Calabrese and J. S. Thompson, *Inorg. Chem.*, 1987, **26**, 1507.
19 G. M. Sheldrick, *Acta Crystallogr., Sect. A*, 1990, **46**, 467.
20 G. M. Sheldrick, SHELXL-97, Program for the refinement of crystal structures, University of Göttingen, 1997.